IEEE Access
Multidisciplinary | Rapid Review | Open Access Journal

Received February 29, 2020, accepted March 23, 2020, date of publication April 6, 2020, date of current version April 22, 2020.

Digital Object Identifier 10.1109/ACCESS.2020.2985849

A Novel Six-Probe Method for the Measurement and Exact Reconstruction of a Pair of Parallel Profiles

XI CHEN, CHANGKU SUN, LUHUA FU, AND CHANGJIE LIU
State Key Laboratory of Precision Measuring Technology and Instruments, Tianjin University, Tianjin 300072, China
Corresponding author: Changjie Liu (liuchangjie@tju.edu.cn)

This work was supported in part by the National Science and Technology Major Project of China under Grant 2016ZX04003001, and in part by the High-Tech Ship Research Project (First Phase of Low-Speed Marine Engine Engineering).

ABSTRACT A novel system and its corresponding method for the measurement and the exact reconstruction of a pair of parallel profiles are designed. There are six sensors installed on the measuring device and they are divided into two groups with different sensor spacings. The exact reconstruction can be realized under the condition of a high lateral resolution, as the straightness error, the yaw error, the zero-adjustment error, and the data processing error can be all eliminated through two scannings and certain data processing method. The measurement error of the displacement sensors can also be suppressed. The new method has the following advantages: (i) the realization of the exact reconstruction, (ii) a high lateral resolution of the reconstruction result which is independent of the sensor spacings, (iii) the skip of the zero calibration before the measurement process, and (iv) the suppression of the sensor random error. These advantages are demonstrated by the theoretical analyses and the simulations. Experiments are also conducted to prove some of these characteristics.

INDEX TERMS Data processing error, error elimination, exact reconstruction, high lateral resolution.

I. INTRODUCTION

The guiding devices, such as a set of guide-ways or parallel plates in equipment, are generally regarded as a pair of parallel profiles whose accuracy greatly influences the smoothness and service life of the devices. Therefore, monitoring the main parameters of a pair of parallel profiles (including distance, straightness, and parallelism *et al*) is of significance proposition. The most commonly used method to address this problem is the scanning measurement method. However, the most remarkable disadvantage of this method is the inevitable errors introduced into the measurement and reconstruction results because the motion trajectory of the measuring device is always used as the measurement reference. Especially for the on-machine measurement, as the measuring device is driven by the machine tool spindle, the accuracy of the measurement reference is always at the same level as the accuracy of the measured profiles, thus impacting on the measurement and reconstruction results more seriously. Therefore, people are working on the researches and the developments of the measurement and reconstruction methods to eliminate different errors in scanning measurement, wherein the multi-sensor method can achieve fairly good results. The main errors that influence the accuracies of the measurement and reconstruction results include the straightness error and the yaw error of the measurement reference, the data processing error, the zero-adjustment error, and the measurement error of sensors. In general, the exact reconstruction of measurement profiles needs to eliminate all of these errors except the sensor measurement error.

For the measurement and reconstruction of a single measured profile, the reversal method using a single displacement sensor can overcome the systematic error in the straightness error of the measurement reference [1], [2]. With two side-by-side sensors, the two-point method [3]–[7], including the sequential two-point method (STP), the generalized two-point method (GTP) and the combined two-point method (CTP), can remove both the systematic error and the random error of the straightness error, but it will amplify the influence of the yaw error of the measuring device at the same time. Correspondingly, the three-point method, including the sequential three-point method (STRP), the generalized

The associate editor coordinating the review of this manuscript and approving it for publication was Zhixiong Peter Li.

three-point method (GTRP) and the combined three-point method (CTRP), can eliminate the yaw error [8], but the zero-adjustment error will have a relatively large impact on the reconstruction result. And if the measurement and reconstruction of the profile are performed by the two-point method or the three-point method when the step distance of the measuring device (equal to the interval of the sampling points and of the reconstruction points) is equal to the spacing between adjacent sensors, which is called the ''shear'', the method is STP or STRP, and the positions of the reconstruction points are not affected by the data processing error. Nevertheless, the density of the sampling points is limited by the size of the sensors and the lower lateral resolution will result in fewer reconstruction points, which makes the features of the measured profile more likely to be lost. In the GTP and GTRP methods, the interval of the sampling points can be smaller than the shear, which improves the lateral resolution. However, as the higher-order harmonic component distortion exists, the results in this method suffer from the data processing error. The CTP method combines the STP and the GTP methods, and the CTRP method blends the STRP and the GTRP methods. Using these two methods, the reconstruction result without data processing error can be obtained under a high lateral resolution theoretically, but in order to adjust the relative positions of the different groups of reconstruction points, these methods assume a completely smooth part of the measured profile, which limits the feasibility and the accuracy of the measurement result. Thus, it is hard to realize the exact reconstruction without data processing error and retain a high lateral resolution at the same time.

Several methods have been developed to remove the data processing error under a high lateral resolution [9]–[12]. However, many of these methods are still affected by the zero-adjustment error of sensors. Yin *et al*. developed new methods including time domain method and frequency domain method [13], [14], which can retain a high lateral resolution without the intervention of data processing error or zero-adjustment error in the reconstruction result. However, if the influence of yaw error is to be overcome, an additional collimator is required to measure the yaw error. Using an interferometer as multiple sensors, they also developed a new method to eliminate both the straightness error and the yaw error and realize the exact reconstruction with a high lateral resolution [15]. Clemens Elster *et al*. developed a new method [16], [17] which combines a multi-sensor system with a laser collimator to eliminate several errors that have major impacts on the reconstruction results, including straightness error and yaw error of the measurement reference and the zero-adjustment error. And with a high lateral resolution, the method is also free from the data processing error, which means the exact reconstruction can be achieved. However, both the interferometer which is used to implement the same function of multiple sensors and the collimator are optical instruments, which require complicated installation and adjustment processes as well as professional operators' operations. Moreover, the stability of the optical instruments is easily affected by the environments, including temperature, humidity, and vibrations *et al*. These factors all limit the feasibility of the measurement systems with the optical instruments in the industrial sites for the complexity of the environment. Besides, some vision measurement methods and image processing technologies are developed, and the measurement accuracy is getting higher and higher. However, for the on-machine measurement, the camera calibration and changes in ambient light all limit the feasibility of these methods, and image stitching is often needed when measuring large-scale workpieces.

Based on the single profile measurement and reconstruction methods described above, many methods for parallel profiles have been developed, including methods for measuring cylinder workpieces and parallel guideways [18]–[21]. The advantages and disadvantages of these methods are similar to those for a single profile. In order to realize the exact reconstruction, the straightness error and the yaw error of the measurement reference, the data processing error, and the zero-adjustment error all need to be eliminated. To ensure the measurement accuracy in the industrial sites, the optical instruments also need to be forbidden. For a better measurement result, a high lateral resolution is needed. Therefore, in this paper, we developed a six-probe system, which uses six displacement sensors to collect data for the measurement and the reconstruction of a pair of parallel profiles. The new method can eliminate several errors mentioned above and realize the exact reconstruction with a high lateral resolution if the sensor measurement error is ignored. At the same time, this method has better stability in complex environments as no optical instruments are used. Moreover, benefiting from the average effect, the sensor measurement error can be suppressed better.

II. THE SIX-PROBE METHOD

A. THE STRUCTURE OF THE MEASUREMENT SYSTEM

To eliminate the straightness error of the reference in the z-direction (referred as straightness error hereinafter) and the yaw error at the same time without using an additional device to measure the yaw error, each measured profile needs to be reconstructed using measurement data of at least three probes side by side. Therefore, the measuring device proposed here consists of six displacement sensors. As shown in Fig.1, the device is mounted on a mobile stage and placed between two measured profiles. The sensors P_1, P_2, and P_3 are mounted on the one side of the stage, and P_4, P_5, and P_6 are fixed on the other side. P_4 is opposite to P_1. Set the symmetry point of P_1 and P_4 as the origin of the coordinate, and the motion direction of the device, which is also the extension direction of the measured profiles, as the positive direction of the x-axis. During the scanning, after the measuring device stepped s each time, sensors collect displacement data once.

It is required to satisfy $d_1 = \delta_1 \cdot s$ and $d_2 = \delta_2 \cdot s$, where δ_1 and δ_2 are coprime (the following analyses are performed under the setting of $\delta_1 > \delta_2$). Both the measured profiles can

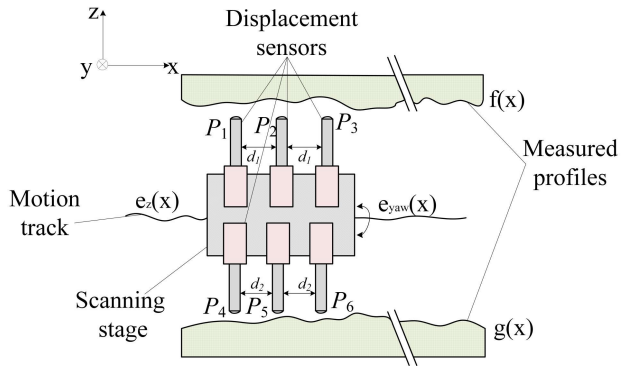

FIGURE 1. The schematic diagram of the six-probe method.

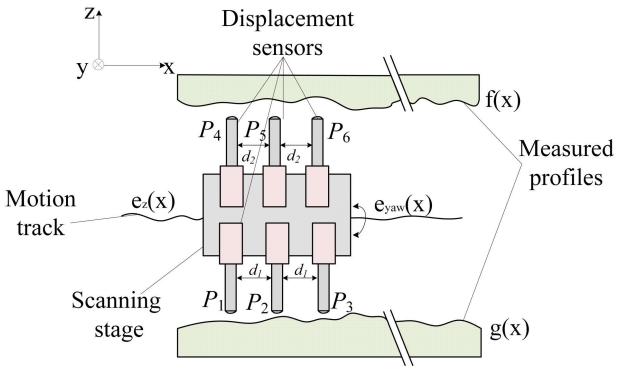

FIGURE 2. The schematic of the scanning after rotation.

be reconstructed by the three-point method using the outputs of P_1 -P_3 and P_4-P_6 after one scanning. According to the existing theories, the three-point method can eliminate the straightness error and the yaw error effectively.

B. THE ELIMINATION OF THE ZERO-ADJUSTMENT ERROR

According to the existing researches, almost all the multi-probe methods include a differential process and an integral process. When reconstructing a measured profile using the three-point method, the reference error (including the straightness error and the yaw error) can be eliminated during the differential process. However, there are errors in differential values as the zero-adjustment error exists. In order to reduce this impact, a higher precision reference plane is often used to calibrate the zero points of sensors, which improves the cost but fails to meet the requirements sometimes, as the integral process is an iterative process which means the errors in differential values accumulate rapidly and even small errors can make a harmful influence on the reconstruction result. Therefore, when the requirement for zero calibration accuracy becomes higher, it is necessary for the measurement and reconstruction method to lessen the influence of zero-adjustment errors, so that not only the measurement accuracy can be improved, the cost can also be reduced as the calibration of sensor zero points is spared.

Using the new method described in this paper, the zero-adjustment error can be removed during the differential part before the integral part. The measuring device is rotated around the x-axis for a second scanning (as shown in Fig.2), with the same start point, end point, and the stepping distance as the first scanning in Fig.1.

Define the two measured profiles as $f(x)$ and $g(x)$ respectively. When the measurement data are collected N times in one scanning, the outputs of $P_j(j = 1, 2, \ldots, 6)$ can be expressed as $m_j(x_n)$, where $n = 0, 1, 2, \ldots, N-1$ and $x_n = n \cdot s$. Set the zero-adjustment error of P_j to e_j. In the first scanning, when the output of P_j is $m_j(x_n)$, the straightness error is expressed as $e_z(x_n)$, and the yaw error of the measuring device is $e_{yaw}(x_n)$. In the second scanning, the measurement data are defined as $m_{jr}(x_n)$, and the straightness error and the yaw error are $e_{zr}(x_n)$ and $e_{yawr}(x_n)$. Considering the straightness error, the yaw error and the zero-adjustment error, the outputs of sensors in two scannings are:

$$m_1(x_n) = f(x_n) - e_z(x_n) + e_1 \tag{1}$$
$$m_2(x_n) = f(x_n + d_1) - e_z(x_n) - d_1 \cdot e_{yaw}(x_n) + e_2 \tag{2}$$
$$m_3(x_n) = f(x_n + 2d_1) - e_z(x_n) - 2d_1 \cdot e_{yaw}(x_n) + e_3 \tag{3}$$
$$m_4(x_n) = -[g(x_n) - e_z(x_n)] + e_4 \tag{4}$$
$$m_5(x_n) = -[g(x_n + d_2) - e_z(x_n) - d_2 \cdot e_{yaw}(x_n)] + e_5 \tag{5}$$
$$m_6(x_n) = -[g(x_n + 2d_2) - e_z(x_n) - 2d_2 \cdot e_{yaw}(x_n)] + e_6 \tag{6}$$
$$m_{1r}(x_n) = -[g(x_n) - e_{zr}(x_n)] + e_1 \tag{7}$$
$$m_{2r}(x_n) = -[g(x_n + d_1) - e_{zr}(x_n) - d_1 \cdot e_{yawr}(x_n)] + e_2 \tag{8}$$
$$m_{3r}(x_n) = -[g(x_n + 2d_1) - e_{zr}(x_n) - 2d_1 \cdot e_{yawr}(x_n)] + e_3 \tag{9}$$
$$m_{4r}(x_n) = f(x_n) - e_{zr}(x_n) + e_4 \tag{10}$$
$$m_{5r}(x_n) = f(x_n + d_2) - e_{zr}(x_n) - d_2 \cdot e_{yawr}(x_n) + e_5 \tag{11}$$
$$m_{6r}(x_n) = f(x_n + 2d_2) - e_{zr}(x_n) - 2d_2 \cdot e_{yawr}(x_n) + e_6 \tag{12}$$

Define the differential value with different selections of x increment as:

$$f_1''(x_n) = \frac{1}{d_1^2}[f(x_n + 2d_1) - 2f(x_n + d_1) + f(x_n)] \tag{13}$$
$$f_2''(x_n) = \frac{1}{d_2^2}[f(x_n + 2d_2) - 2f(x_n + d_2) + f(x_n)] \tag{14}$$
$$g_1''(x_n) = \frac{1}{d_1^2}[g(x_n + 2d_1) - 2g(x_n + d_1) + g(x_n)] \tag{15}$$
$$g_2''(x_n) = \frac{1}{d_2^2}[g(x_n + 2d_2) - 2g(x_n + d_2) + g(x_n)] \tag{16}$$

The calculation process of the second-order differentials that are not affected by the zero error is:

$$\begin{aligned} df_1(x_n) &= \frac{1}{d_1^2}[m_3(x_n) - 2m_2(x_n) + m_1(x_n)] \\ &= f_1''(x_n) + \frac{1}{d_1^2}(e_3 - 2e_2 + e_1) \end{aligned} \tag{17}$$

$$df_{1r}(x_n) = \frac{1}{d_1^2}\{m_{1r}(x_n + 2d_1) + m_{4r}(x_n + 2d_1)$$

$$
\begin{aligned}
&-m_{3r}(x_n) - 2[m_{1r}(x_n + d_1)\\
&+m_{4r}(x_n + d_1)\\
&-m_{2r}(x_n)]\\
&+m_{4r}(x_n)\}\\
&= f_1''(x_n) - \frac{1}{d_1^2}(e_3 - 2e_2 + e_1) \qquad (18)
\end{aligned}
$$

$$
\begin{aligned}
df_2(x_n) = &\frac{1}{d_2^2}\{m_1(x_n + 2d_2) + m_4(x_n + 2d_2)\\
&-m_6(x_n) - 2[m_1(x_n + d_2)\\
&+m_4(x_n + d_2)\\
&-m_5(x_n)] + m_1(x_n)\}\\
&= f_2''(x_n) - \frac{1}{d_2^2}(e_6 - 2e_5 + e_4) \qquad (19)
\end{aligned}
$$

$$
\begin{aligned}
df_{2r}(x_n) = &\frac{1}{d_2^2}[m_{6r}(x_n) - 2m_{5r}(x_n) + m_{4r}(x_n)]\\
&= f_2''(x_n) + \frac{1}{d_2^2}(e_6 - 2e_5 + e_4) \qquad (20)
\end{aligned}
$$

The second-order differential values of $f(x)$ with x increments of d_1 and d_2 are:

$$mf_1(x_n) = \frac{1}{2}[df_1(x_n) + df_{1r}(x_n)] = f_1''(x_n) \qquad (21)$$

$$mf_2(x_n) = \frac{1}{2}[df_2(x_n) + df_{2r}(x_n)] = f_2''(x_n) \qquad (22)$$

Similarly, with x increments of d_1 and d_2, the calculation process of the second-order differentials of $g(x)$ ($mg_1(x_n)$ and $mg_2(x_n)$), can be calculated:

$$
\begin{aligned}
mg_1(x_n) = &-\frac{1}{2d_1^2}\{m_1(x_n + 2d_1) + m_4(x_n + 2d_1)\\
&-m_3(x_n) - 2[m_1(x_n + d_1)\\
&+m_4(x_n + d_1)\\
&-m_2(x_n)]\\
&+m_4(x_n) + m_{3r}(x_n)\\
&-2m_{2r}(x_n) + m_{1r}(x_n)\}\\
&= g_1''(x_n) \qquad (23)
\end{aligned}
$$

$$
\begin{aligned}
mg_2(x_n) = &-\frac{1}{2d_2^2}\{m_6(x_n) - 2m_5(x_n) + m_4(x_n)\\
&+m_{1r}(x_n + 2d_2)\\
&+m_{4r}(x_n + 2d_2)\\
&-m_{6r}(x_n) - 2[m_{1r}(x_n + d_2)\\
&+m_{4r}(x_n + d_2)\\
&-m_{5r}(x_n)]\\
&+m_{1r}(x_n)\}\\
&= g_2''(x_n) \qquad (24)
\end{aligned}
$$

We can see that the differential values in (21)-(24) are free from the zero-adjustment error. The reconstruction result calculated from these values will not be impacted by this type of error.

C. THE RECONSTRUCTION OF THE MEASURED PROFILES

As the differential process in Section II(B) eliminates the zero-adjustment error, the differential values can be used in the integral process without worrying about the accumulation of this type of error. To meet the measurement requirements and realize the exact reconstruction of profiles without data processing error, the number of measurement points N needs to be at least $2\delta_1\delta_2$, that is to say, the measurement length is at least $L = (2\delta_1\delta_2 - 1)s$. When $n = 0, 1, 2, \ldots, N-1$, $f(x_n)$ is represented by $f(n)$ for the convenience of representation.

Using $x_\alpha, \alpha = 0, 1, 2, \ldots, \delta_1 - 1$ as the starting point and $mf_1(x_n)$, conduct δ_1 sets of double integrals with x increment of d_1 (the STRP method). It will result in δ_1 reconstruction profiles with at least $2\delta_2$ reconstruction points on each profile. Similarly, using $x_\beta, \beta = 0, 1, 2, \ldots, \delta_2 - 1$ as the starting point and $mf_2(x_n)$, conduct δ_2 sets of double integrals with x increment of d_2, and δ_2 reconstruction profiles with at least $2\delta_1$ reconstruction points on each profile can be obtained. The integral processes can be implemented by:

$$f_1'(x_i) = f_1''(x_{i-\delta_1}) \cdot d_1 + f_1'(x_{i-\delta_1}) \qquad (25)$$

$$f_1(x_i) = f_1'(x_{i-\delta_1}) \cdot d_1 + f_1(x_{i-\delta_1}) \qquad (26)$$

$$f_2'(x_i) = f_2''(x_{i-\delta_2}) \cdot d_2 + f_2'(x_{i-\delta_2}) \qquad (27)$$

$$f_2(x_i) = f_2'(x_{i-\delta_2}) \cdot d_2 + f_2(x_{i-\delta_2}) \qquad (28)$$

We define a pair of measured profiles, and simulating the data collection and the data processing processes, one of the measured profiles and $\delta_1 + \delta_2$ profiles calculated from (25)-(28) of it are shown in Fig. 3 and Fig. 4 (here we define $\delta_1 = 11, \delta_2 = 9$).

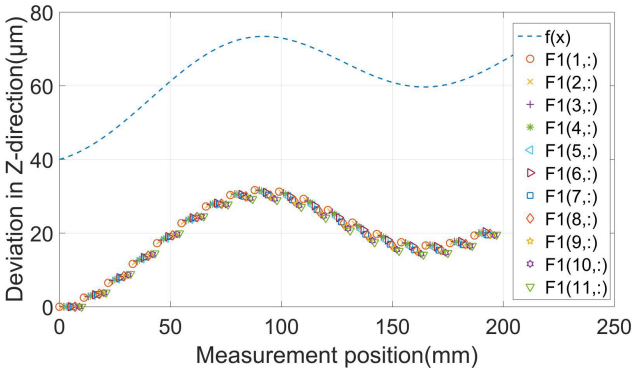

FIGURE 3. δ_1 profiles with a reconstruction point interval of d_1.

Since the mentioned reconstruction profiles are obtained by the STRP method, the two groups of profiles with point intervals of d_1 and d_2 are not affected by the data processing error. However, due to the selections of the initial values in iterations (all selected as 0 here), the reconstruction profiles have tilts and translations compared with the actual profile, and for each profile, the tilt and the translation are always different from others'. Adjusting the poses of these reconstruction profiles by rotating and translating them, each group of reconstruction profiles can construct a whole profile with

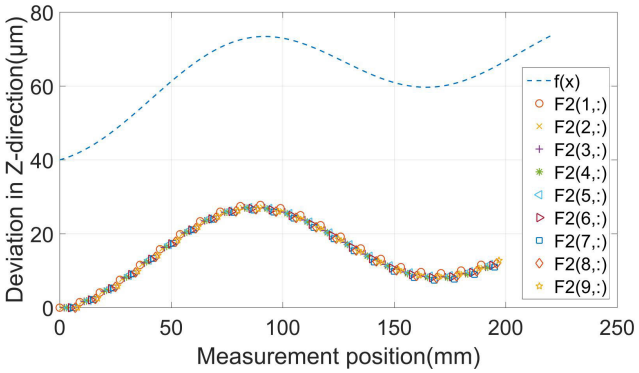

FIGURE 4. δ_2 profiles with a reconstruction point interval of d_2.

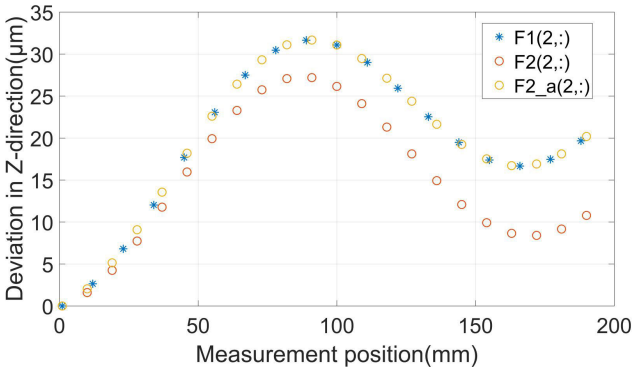

FIGURE 5. The adjustment of the reference profile.

the reconstruction point interval of s and more than $2\delta_1\delta_2$ reconstruction points.

Store the reconstruction values of points on these profiles in arrays F_1 and F_2. Define $rem(a, b)$ as the remainder of a divided by b, and $floor(a)$ as the largest integer not bigger than a. When $r_j = rem(n, \delta_j)$, $t_j = floor(n/\delta_j)$, set $F_j(r_j+1, :)$ as the $(r_j + 1)$th profile of the profile group which consists of profiles with point interval of d_j, and $F_j(r_j + 1, t_j + 1)$ as the $(t_j + 1)$th point on it, whose x coordinate is $x_n = ns$. When the tangent of the angle of which $F_j(r_j + 1, :)$ relative to the actual profile $f(x)$ is defined as $k_j(r_j + 1)$, the reconstruction points on $F_j(r_j + 1, :)$ can be expressed as:

$$F_j(r_j + 1, t_j + 1) = f(n) + k_j(r_j+1)\cdot(n - r_j)s - f(r_j) \quad (29)$$

In the process of adjusting reconstruction profiles, when using $F_1(p + 1, :), p = 0, 1, 2, \ldots, \delta_1 - 1$ as the target profile, other profiles in F_1 need to be adjusted to coincide with the target profile, and $F_2(q + 1, :), q = rem(p, \delta_2)$ should be used as the reference profile. We know that, in the measurement positions of $n_0 = p$ and $n_0' = p + \delta_1\delta_2$ ($x = n_0 s$ and $x = n_0' s$), there are reconstruction points on both $F_1(p + 1, :)$ and $F_2(q + 1, :)$. Rotating and translating $F_2(q + 1, :)$, the result is $F_2\_a(q + 1, :)$ and the purpose of this operation is to make the points on $F_2\_a(q + 1, :)$ and $F_1(p+1, :)$ coincide in two mentioned positions where $n = n_0$ and $n = n_0'$. Next, make other profiles in F_1 also coincide with $F_2\_a(q + 1, :)$ and $F_1(p + 1, :)$, and this process takes the points on $F_2\_a(q+1, :)$ as references. There are δ_1 profiles in F_1 and at least $2\delta_1$ points on $F_2\_a(q+1, :)$. In each profile in F_1, there are two reconstruction positions where there are points on $F_2\_a(q + 1, :)$ as well.

For example, we use the 2nd reconstruction profile in F_1, the points on which are expressed as $F_1(2, i_1), i_1 = 1, 2, \cdots, 2\delta_2, \cdots$, as the target profile when adjusting the relative positions and poses among profiles in F_1. According to the introduction above, the reference profile should be $F_2(2, :)$ (with points $F_2(2, i_2), i_2 = 1, 2, \ldots, 2\delta_1, \ldots$). The values of reconstruction points on these two profiles are:

$$F_1(2, i_1) = f(n) + k_1(2)\cdot(n - 1)s - f(1), \quad n = (i_1 - 1)\delta_1 + 1 \quad (30)$$

$$F_2(2, i_2) = f(n) + k_2(2)\cdot(n - 1)s - f(1), \quad n = (i_2 - 1)\delta_2 + 1 \quad (31)$$

The two points on $F_2(2, :)$, whose x coordinates satisfy $n_0 = 1$ and $n_0' = 1 + \delta_1\delta_2$, can be used to adjust it to make it coincide with $F_1(2, :)$. In these two positions, both $F_1(2, :)$ and $F_2(2, :)$ has reconstruction points, and according to (30)-(31) the values of these four reconstruction points can be expressed as:

$$F_1(2, 1) = F_2(2, 1) = 0, \quad n = n_0 \quad (32)$$

$$F_1(2, \delta_2 + 1) = f(n_0') + k_1(2)\cdot\delta_1\delta_2\cdot s - f(1), \quad n = n_0' \quad (33)$$

$$F_2(2, \delta_1 + 1) = f(n_0') + k_2(2)\cdot\delta_1\delta_2\cdot s - f(1), \quad n = n_0' \quad (34)$$

Define the slope difference between $F_1(2, :)$ and $F_2(2, :)$ as $\Delta k(0)$:

$$\Delta k(0) = \frac{F_1(2, \delta_2 + 1) - F_2(2, \delta_1 + 1)}{\delta_1\delta_2 s} = k_1(2) - k_2(2) \quad (35)$$

The process of obtaining $F_2\_a(2, i_2)$, which are the points after $F_2(2, :)$ being adjusted, can be expressed as:

$$F_2\_a(2, i_2) = F_2(2, i_2) + \Delta k(0)\cdot(n - 1)\cdot s = f(n) + k_1(2)\cdot(n - 1)\cdot s - f(1) \quad (36)$$

The adjustment process of the reference profile $F_2(2, :)$ in (35)-(36) is shown in Fig 5.

Then adjust the positions and poses of other profiles in F_1 to make them coincide with the target profile $F_1(2, :)$, that is, coincide with the reference profile after adjustment ($F_2\_a(2, :)$). When i_2 takes $i_2 \in \{x | x \in Z, 1 \le x \le \delta_1 \; and \; x \ne 2\}$, each point in $F_2\_a(2, i_2)$ can be used as the reference for the position and pose adjustment of one of profile in F_1. Define that:

$$\hat{n}_1 = (i_2 - 1)\delta_2 + 1$$
$$\hat{n}_2 = (i_2 - 1)\delta_2 + \delta_1\delta_2 + 1$$

When n is equal to $\hat{n}_1$ or $\hat{n}_2$, in the corresponding two positions, the values of points on $F_2\_a(2,:)$ and points in F_1 are expressed as:

$$F_2\_a(2,i_2) = f(\hat{n}_1)+k_1(2)\cdot(\hat{n}_1-1)s-f(1) \quad (37)$$

$$F_2\_a(2,i_2+\delta_1) = f(\hat{n}_2)+k_1(2)\cdot(\hat{n}_2-1)s-f(1) \quad (38)$$

$$F_1(\hat{r}+1,\hat{t}+1) = f(\hat{n}_1)+k_1(\hat{r}+1)\cdot(\hat{n}_1-\hat{r})s-f(\hat{r}) \quad (39)$$

$$F_1(\hat{r}+1,\hat{t}+\delta_2+1) = f(\hat{n}_2)+k_1(\hat{r}+1)\cdot(\hat{n}_2-\hat{r})s-f(\hat{r}) \quad (40)$$

where $\hat{r} = rem(\hat{n}_1,\delta_1)$ and $\hat{t} = floor(\hat{n}_1/\delta_1)$. According to (39)-(40), we know that in F_1, the reconstruction points in these two positions are both on the $(\hat{r}+1)$th reconstruction profile ($F_1(\hat{r}+1,:)$). Define the slope difference between $F_1(\hat{r}+1,:)$ and $F_2\_a(2,:)$ (which is equal to the slope difference between $F_1(\hat{r}+1,:)$ and $F_1(2,:)$) as $\Delta k(\hat{r}+1)$:

$$\begin{aligned}\Delta k(\hat{r}+1) = \frac{1}{\delta_1\delta_2 s}[&F_2\_a(2,i_2+\delta_1)\\ &-F_2\_a(2,i_2)\\ &-F_1(\hat{r}+1,\hat{t}+\delta_2+1)\\ &+F_1(\hat{r}+1,\hat{t}+1)]\\ = k_1(2)-k_1(\hat{r}+1)\end{aligned} \quad (41)$$

The profile $F_1(\hat{r}+1,:)$ is rotated according to the slope difference $\Delta k(\hat{r}+1)$, and the profile after rotation is defined as $F_1\_r(\hat{r}+1,:)$:

$$\begin{aligned}F_1\_r(\hat{r}+1,:) &= F_1(\hat{r}+1,:)+\Delta k(\hat{r}+1)\cdot(n-\hat{r})s\\ &= f(n)+k_1(2)\cdot(n-\hat{r})s-f(\hat{r})\end{aligned} \quad (42)$$

After rotation, we know that $F_1\_r(\hat{r}+1,:)$ and $F_2\_a(2,:)$ are parallel according to (36) and (42). In these two corresponding positions, the values of the reconstruction points on $F_1\_r(\hat{r}+1,:)$ are expressed as:

$$F_1\_r(\hat{r}+1,\hat{t}+1) = f(\hat{n}_1)+k_1(2)\cdot(\hat{n}_1-\hat{r})s-f(\hat{r}) \quad (43)$$

$$F_1\_r(\hat{r}+1,\hat{t}+\delta_2+1) = f(\hat{n}_2)+k_1(2)\cdot(\hat{n}_2-\hat{r})s-f(\hat{r}) \quad (44)$$

The vertical translation between $F_1\_r(\hat{r}+1,:)$ and $F_2\_a(2,:)$ (equal to the translation between $F_1\_r(\hat{r}+1,:)$ and $F_1(2,:)$) is:

$$\begin{aligned}\Delta d(\hat{r}+1) = \frac{1}{2}[&F_2\_a(2,i_2)-F_1\_r(\hat{r}+1,\hat{t}+1)\\ &+F_2\_a(2,i_2+\delta_1)\\ &-F_1\_r(\hat{r}+1,\hat{t}+\delta_2+1)]\\ = k_1(2)\cdot(\hat{r}-1)s+f(\hat{r})-f(1)\end{aligned} \quad (45)$$

According to $\Delta d(\hat{r}+1)$, translate $F_1\_r(\hat{r}+1,:)$ and obtain the profile $F_1\_a(\hat{r}+1,:)$:

$$\begin{aligned}F_1\_a(\hat{r}+1,:) &= F_1\_r(\hat{r}+1,:)+\Delta d(\hat{r}+1)\\ &= f(n)+k_1(2)\cdot(n-1)s-f(1)\end{aligned} \quad (46)$$

The component $k_1(2)\cdot(n-1)s$ is the difference between $F_1\_a(\hat{r}+1,:)$ and the actual profile $f(x)$ due to tilt, and $-f(1)$ is the difference caused by the translation. The expressions of $F_1\_a(\hat{r}+1,:)$ and $F_1(2,:)$ are the same ((30) and (46)), which means that each profile in $F_1\_a(\hat{r}+1,:)$ has the same tilt and translation as $F_1(2,:)$. That is to say, they all coincide with $F_1(2,:)$, and the mentioned result is shown in Fig.6.

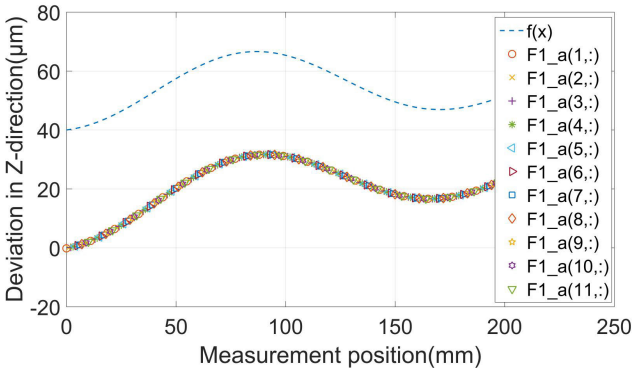

FIGURE 6. The δ_1 reconstruction profiles in F_1 after adjustment.

Therefore, based on the mentioned steps, δ_1 profiles in F_1 could coincide with each other and combine a whole profile with at least $2\delta_1\delta_2$ points and an interval of s. It's an exact reconstruction with a high lateral resolution and without data processing error as all the profiles in F_1 and F_2 are calculated by the STRP method, and the sampling point interval (s) can be controlled independently with the sensor spacing.

Based on the same method, using different reconstruction profiles in F_1 or F_2 as the target profile, different profiles can be obtained. Although they have different tilts and translations compared with the actual profile, after being deprived of the linear trends, they can overlap with each other theoretically if the measurement error of sensors is ignored. When considering the measurement error of sensors, the averaging of them can suppress the random error. The reconstruction profile of the other measured profile $g(x)$ can be calculated using the same method as well. What must be noticed is that when $p \geq \delta_2$, it is needed not only to rotate the profile according to (35)-(36) but also to translate it when adjusting the position and the pose of the reference profile.

D. THE EVALUATION OF THE PARALLELISM

After the steps described in Section II(C), we can obtain two reconstruction profiles without the influence of the straightness error, the yaw error, the zero-adjustment error, and the data processing error. It is equivalent to achieving an exact reconstruction and the reconstruction profiles are similar to the actual profiles, but there are still tilts and translations between the reconstruction profiles and their corresponding actual profiles. These tilts and translations will not affect the evaluation result if the reconstruction profiles are used to evaluate their straightnesses. However, when the tilt angles of these two reconstruction profiles compared with their actual profiles are different from each other, there will be a large impact on the evaluation result of the parallelism. Therefore,

to evaluate the parallelism, adjusting the relative position between the reconstruction profiles obtained in Section II(C) is the basis, so that the angle between them is equal to that between the actual profiles (the angle here refers to the angle between the fitting straight lines of profiles). The method used here is similar to that in [18], and differently, we can calculate the slope difference of profiles using the data from two scannings:

$$\Delta p = \frac{N\sum_{n=0}^{N-1} x_n \cdot m_p(x_i) - \sum_{n=0}^{N-1} x_i \sum_{n=0}^{N-1} m_p(x_i)}{N\sum_{n=0}^{N-1} x_n^2 - \left(\sum_{n=0}^{N-1} x_n\right)^2} \quad (47)$$

where $m_p(x_i) = [m_1(x_n) + m_4(x_n) + m_{1r}(x_n) + m_{4r}(x_n)]/2$. Define that the reconstruction profiles obtained in Section II(C) are $Z_f(x_n)$ and $Z_g(x_n)$, and the slopes of their fitting straight lines are p_f and p_g, the adjustment process is:

$$Z_{fr}(x_n) = Z_f(x_n) + (\frac{\Delta p}{2} - p_f)x_n \quad (48)$$

$$Z_{gr}(x_n) = Z_g(x_n) + (-\frac{\Delta p}{2} - p_g)x_n \quad (49)$$

The angle between $Z_{fr}(x_n)$ and $Z_{gr}(x_n)$ is equal to that between two actual profiles. As a result, $Z_{fr}(x_n)$ and $Z_{gr}(x_n)$ can be used to evaluate both the straightnesses of them and the parallelism.

As the proposed method is based on the STRP method, the final reconstruction result will not be affected by the straightness error and the yaw error of the measurement reference as well as the data processing error. According to Section II(B), the zero-adjustment error of sensors is removed during the differential part of the data processing. That is to say, the new method proposed in this paper can eliminate the main factors that influence the reconstruction results most including the errors mentioned above, and the exact reconstruction can be realized if the measurement error of sensors is ignored. Considering the measurement error of sensors, the mentioned $\delta_1 + \delta_2$ profiles calculated using different target profiles can be averaged to reduce the impact of this type of random error. The reconstruction profiles can be used to evaluate the straightnesses of them. After the rotation expressed above, the profiles can be used to evaluate the parallelism as well.

III. SIMULATIONS

In order to demonstrate and verify the feasibility of the new method proposed in this paper, as well as its advantages in eliminations or suppressions of different types of errors and in the exact reconstruction of a pair of profiles, some simulations about the measurement and reconstruction processes are conducted. Suppose that the measured profiles are composed of smooth profiles and irregular variations. The smooth profiles for measured profiles $f(x)$ and $g(x)$ are expressed as (unit: μm):

$$f_b(x) = 20\sin(2\pi \cdot \frac{0.09}{150} \cdot x) - 20\sin(2\pi \cdot \frac{0.8}{150} \cdot x) + 50$$

$$g_b(x) = -50\sin(2\pi \cdot \frac{0.3}{150} \cdot x) - 10\sin(2\pi \cdot \frac{1.34}{150} \cdot x) - 50$$

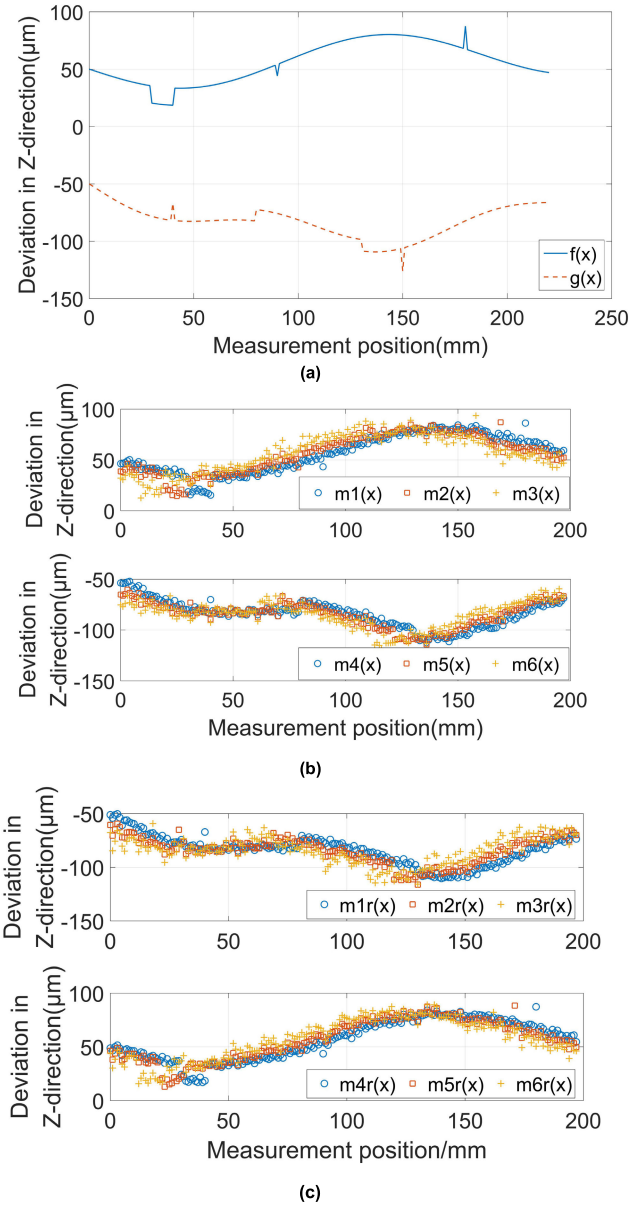

FIGURE 7. The measured profiles and the measurement data: (a) the measured profiles, (b) the measurement data of the first scanning, (c) the measurement data of the second scanning.

Add pulse signals and step variations into the smooth profiles to simulate the irregular variations of the measured profiles, and the whole measured profiles $f(x)$ and $g(x)$ are shown in Fig.7(a). Set d_1, the spacing between P_1-P_3, is 11mm, and 9mm for d_2, the spacing between P_4-P_6. The step distance of the device during the scannings is 1mm. That is to say, the two coefficients (δ_1 and δ_2) are 11 and 9, respectively.

In order to compare the performances of the new method described in this paper and the existing methods, the measurement data of six sensors are processed by different methods to reconstruct the measured profiles.

A. THE ELIMINATION OF THE DATA PROCESSING ERROR

In the two scannings before and after the rotation, add Gaussian error with the standard deviation of $2\mu m$ as the

straightness error of the measurement reference into simulations, as well as yaw errors with the standard deviation of $5\mu rad$. The outputs of six sensors reflect the tendency of measured profiles and are impacted by different types of errors. The measured profiles and the outputs of sensors are shown in Fig.7(b)(c):

Firstly, the simulations are conducted without adding the zero-adjustment error and the measurement error of the sensors. Using the outputs of P_1-P_3 during the first and the second scanning, the reconstruction result in Fig.8(a) is calculated by the STRP method. From Fig.8(a), we can see that the STRP method can realize exact reconstruction ignoring the zero-adjustment error and the measurement error of sensors, as each point on the reconstruction profiles coincides with the measured profiles. However, the interval among the reconstruction points is limited by the shear value, and due to the large interval, a lot of information cannot be displayed on the reconstruction profiles.

Using outputs of six sensors during the first scanning and the GTRP method, the reconstruction profiles are shown in Fig.8(b). That is to say, $Z_f\_gtrp(x)$, the reconstruction profile of $f(x)$, is calculated by a GTRP process with the shear value of $11mm$ and the sampling interval of $1mm$, and $Z_g\_gtrp(x)$ is calculated by a GTRP process with the shear value of $9mm$ and the sampling interval of $1mm$. According to the existing researches, as the GTRP method can overcome the straightness error and the yaw error of the measurement reference, the differences between the measured profiles and the reconstruction profiles shown in Fig.8(b) are caused by data processing error of the method.

What is shown in Fig.8(c) is the reconstruction result calculated using outputs of sensors during two scannings and the new method proposed in this paper. Compared with Fig.8(a) and Fig.8(b), the new method can realize the exact reconstruction and retain a high lateral resolution.

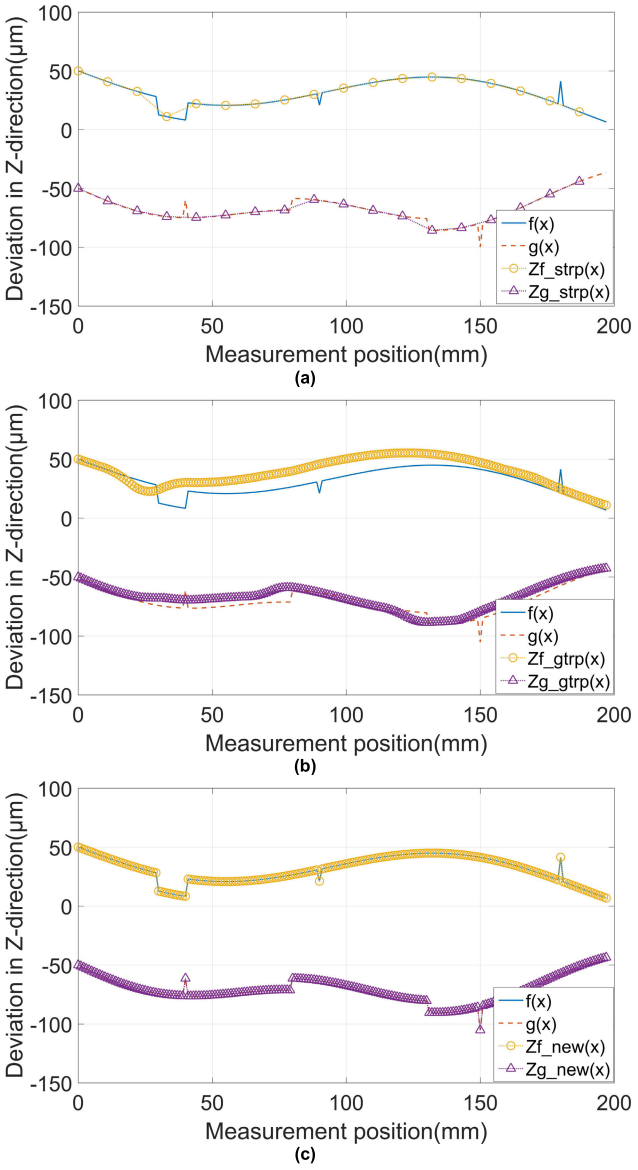

FIGURE 8. The reconstruction result using different methods (ignoring the zero-adjustment error and removing the linear trends of profiles): (a) the reconstruction result of the STRP method, (b) the reconstruction result of the GTRP method, (c) the reconstruction result of the new method.

B. THE ELIMINATION OF THE ZERO-ADJUSTMENT ERROR

Set that all of the sensors have zero-adjustment error not more than 0.5μm when installing. Reconstruct the profiles using the same three methods in Section III(A), and the reconstruction results are shown in Fig.9. Compared with the results in Section III(A), the accuracies of reconstructions will be seriously impacted when using traditional STRP and GTRP methods. The new method removes this influence during the data processing process, which is consistent with the analyses in Section II(B). Therefore, using the new method, the calibration of the sensor zero points can be skipped. As a result, the new method not only ensures the accuracy of the measurement and reconstruction but also simplifies some steps in the measurement process.

C. THE SENSOR MEASUREMENT ERROR SUPPRESSION OF AVERAGE EFFECT

As the reference errors (including the straightness error and the yaw error), the zero-adjustment error and the data processing error are all removed, the error that affects the final result most is the measurement error of sensors. According to the descriptions in Section II(C), using different profiles as the reference profile when adjusting other profiles, different profiles can be obtained. When the average profile is calculated by averaging these different reconstruction profiles, the average effect can suppress the sensor measurement error to some degree. Assume that the measurement error of each displacement sensor is Gaussian error with the standard deviation of $2\mu m$ and add them into sensor outputs, the comparison before and after the averaging is shown in Fig.10. Fig.10(a) shows $Z_f\_1(x)$, using $F_1(1,:)$ as the reference profile when adjusting other profiles, and $Z_f\_average(x)$ is the result of the profile averaging 20 $(\delta_1 + \delta_2)$ reconstruction profiles obtained by using different profiles as reference profile. Fig.10(b) shows

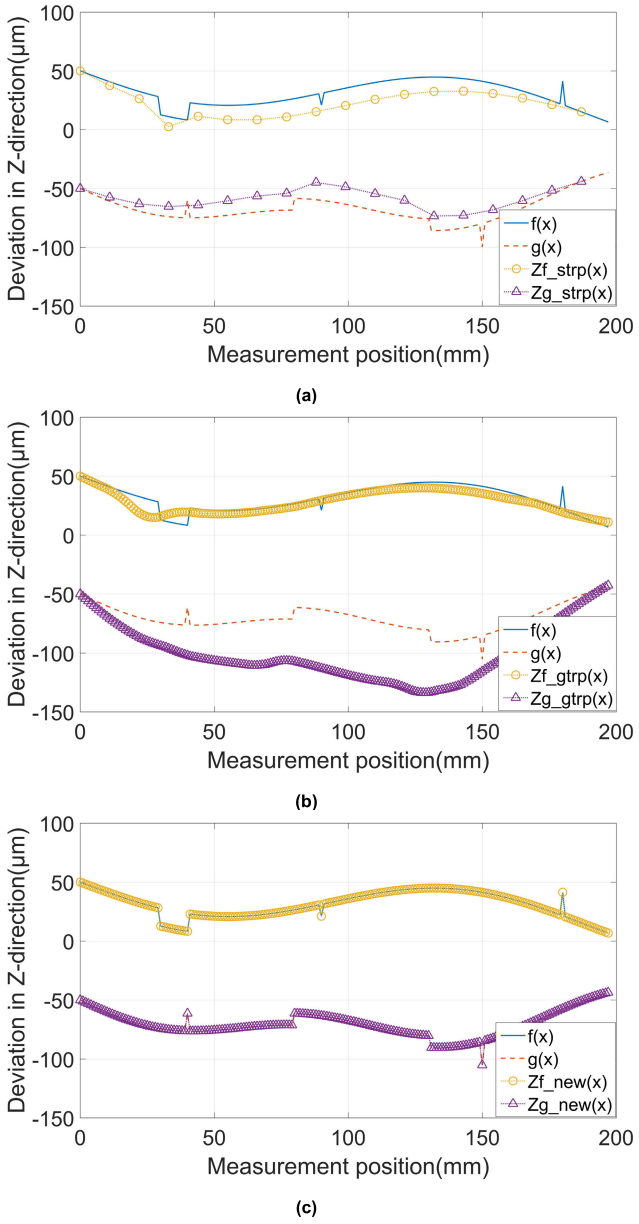

FIGURE 9. The reconstruction results using different methods considering the zero-adjustment error (ignoring the sensor measurement error and depriving the linear trends of profiles): (a) the reconstruction result of the STRP method, (b) the reconstruction result of the GTRP method, (c) the reconstruction result of the new method.

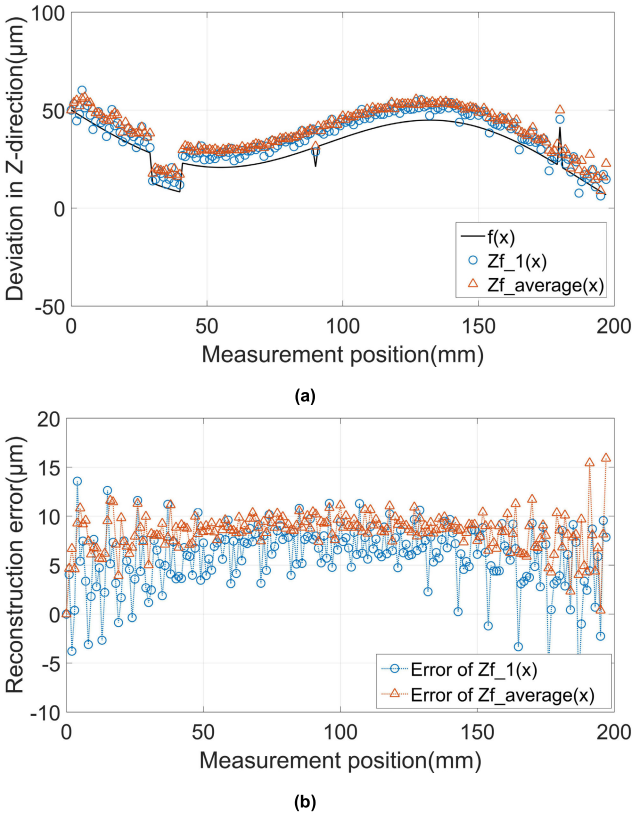

FIGURE 10. The sensor measurement error suppression of average effect: (a) A single reconstruction profile and the average reconstruction profile, (b) Reconstruction errors of profiles in (a).

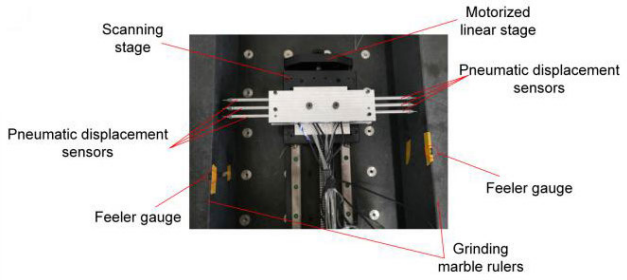

FIGURE 11. Experimental device.

their corresponding reconstruction errors. It can be seen that the average effect suppresses the measurement error of the sensors.

IV. EXPERIMENT

The following experiment was conducted to verify the advantages of the new method. As shown in Fig.11, install six pneumatic displacement sensors (Solartron DP/10/P) with a measurement range of 10mm on the scanning stage. The spacing between P_1-P_3 was 16mm (d_1), and 14mm (d_2) for the other three sensors. The measured objects were a pair of grinding marble rulers, and two feeler gauges of thickness 0.5mm and 0.3mm were attached to the marble rulers to simulate step variations on the measured profiles. The device, driven by a motorized linear stage, collected measurement data after stepping every 2mm. According to the mentioned analyses, δ_1 and δ_2 were equal to 8 and 7. Before and after the measuring device was rotated, two scanning measurements were performed to complete one measurement process, and each scanning needed to collect at least 112 times of measurement data.

In order to verify the performance and advantages of the new method under high lateral resolution, the data collected from the same measurement process was processed by different methods, and the reconstruction results were compared. We know that the results of the three-point method are free from the straightness error and the yaw error, and we compare

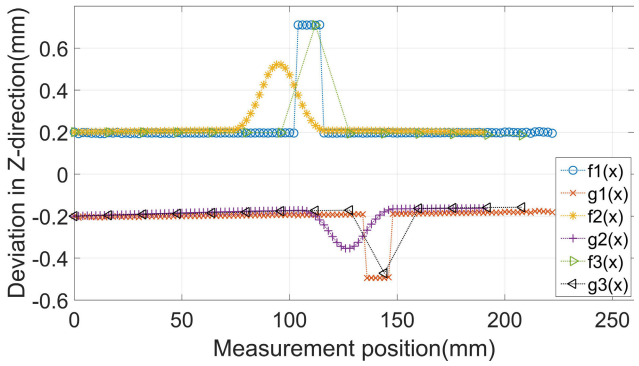

FIGURE 12. The reconstruction results of different methods (the new method, the GTRP method, and the STRP method).

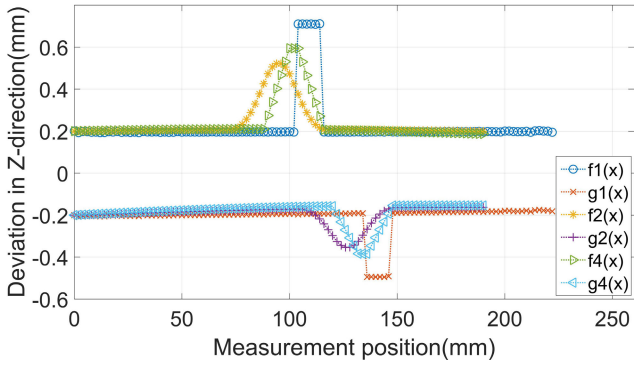

FIGURE 13. The reconstruction results of different methods (the new method, the GTRP method, and the GTP method).

the result of the new method with that of the traditional STRP and the GTRP methods. As shown in Fig.12, using the new method proposed in this paper and the measurement data of two scannings, the reconstruction result of two measured profiles are f_1 and g_1. f_2 and g_2 are reconstruction result calculated from the data of P_1-P_4 and the GTRP method, and f_3 and g_3 are obtained by the STRP method. The main purpose here is to compare their abilities to eliminate the data processing error, as a result, when using the GTRP and the STRP method, the zero-adjustment error is eliminated by the theory in Section II(B). Actually, besides the limitation shown in Fig.12 and Fig.13, their reconstruction results are also be affected by the zero-adjustment error seriously. f_4 and g_4 in Fig.13 are calculated from the data of P_1 and P_2 and the GTP method. It is obvious that f_3 and g_3 have fewer reconstruction points as the low lateral resolution of the STRP method. Some features are missed, that why a high lateral resolution is required. The other three reconstruction profiles all have high lateral resolutions. Comparing the reconstruction results of feeler gauge edges on f_2, and f_4 with that on f_1, the stepwise variations are smoothed by the data processing error when using the GTRP and the GTP method. Therefore, the experiment results show that compare with several traditional methods mentioned above, the new method has a better performance when measuring and reconstructing the profiles with a high lateral resolution.

As expressed in Section III(C), the influence of the measurement error of the sensors can be suppressed through the averaging of the reconstruction profiles which are calculated using different reference profiles. Evaluating the straightnesses of the profiles which is constituted of the first 50 reconstruction points (without additional step variations), the straightness of f_1 in Fig.13 is $7.66\mu m$, and that of a single profile without averaging is $40.10\mu m$. We know that the marble rulers used here have a straightness less than $10\mu m$, thus the suppression of the measurement error is effective.

V. CONCLUSION

A new six-probe system and its corresponding method for the measurement and the reconstruction of a pair of parallel profiles are introduced in this paper. Sensors collect measurement data during two scannings before and after a rotation of the measuring device. Several reconstruction profiles can be obtained using the measurement data and the STRP method. After the adjustments of these profiles, they can combine whole profiles and the exact reconstruction can be realized. The reference error (the straightness error and the yaw error) and the zero-adjustment error can be eliminated during the data processing process. The data processing error can be overcome while a high lateral resolution can be retained. The measurement error of sensors can be suppressed due to the average effect.

REFERENCES

[1] W. T. Estler, "Calibration and use of optical straightedges in the metrology of precision machines," *Opt. Eng.*, vol. 24, no. 3, Jun. 1985.
[2] A. Campbell, "Measurement of lathe Z-slide straightness and parallelism using a flat land," *Precis. Eng.*, vol. 17, no. 3, pp. 207–210, Jul. 1995.
[3] S. Kiyono and W. Gao, "Profile measurement of machined surface with a new differential method," *Precis. Eng.*, vol. 16, no. 3, pp. 212–218, Jul. 1994.
[4] H. Tanaka, K. Tozawa, H. Sato, M. O-Hori, H. Sekiguchi, and N. Taniguchi, "Application of a new straightness measurement method to large machine tool," *CIRP Ann.*, vol. 30, no. 1, pp. 455–459, Jan. 1981.
[5] W. Gao and S. Kiyono, "High accuracy profile measurement of a machined surface by the combined method," *Measurement*, vol. 19, no. 1, pp. 55–64, Sep. 1996.
[6] K. Tozawa, H. Sato, and M. O-Hori, "A new method for the measurement of the straightness of machine tools and machined work," *J. Mech. Des.*, vol. 104, no. 3, pp. 587–592, Jul. 1982.
[7] H. Tanaka and H. Sato, "Extensive analysis and development of straightness measurement by Sequential-Two-Points method," *J. Eng. Ind.*, vol. 108, no. 3, pp. 176–182, Aug. 1986.
[8] W. Gao and S. Kiyono, "On-machine profile measurement of machined surface using the combined three-point method," *JSME Int. J. C Mech. Syst., Mach. Elements Manuf.*, vol. 40, no. 2, pp. 253–259, Feb. 1997.
[9] I. Weingärtner and C. Elster, "System of four distance sensors for high-accuracy measurement of topography," *Precis. Eng.*, vol. 28, no. 2, pp. 164–170, Apr. 2004.
[10] E. H. K. Fung and S. M. Yang, "An error separation technique for measuring straightness motion error of a linear slide," *Meas. Sci. Technol.*, vol. 11, no. 10, pp. 1515–1521, Oct. 2000.
[11] E. H. K. Fung and S. M. Yang, "An approach to on-machine motion error measurement of a linear slide," *Measurement*, vol. 29, no. 1, pp. 51–62, Jan. 2001.
[12] S. M. Yang, E. H. K. Fung, and W. M. Chiu, "Uncertainty analysis of on-machine motion and profile measurement with sensor reading errors," *Meas. Sci. Technol.*, vol. 13, no. 12, pp. 1937–1945, Dec. 2002.
[13] Z.-Q. Yin and S.-Y. Li, "Exact straightness reconstruction for on-machine measuring precision workpiece," *Precis. Eng.*, vol. 29, no. 4, pp. 456–466, Oct. 2005.

[14] Z.-Q. Yin and S.-Y. Li, "High accuracy error separation technique for on-machine measuring straightness," *Precis. Eng.*, vol. 30, no. 2, pp. 192–200, Apr. 2006.
[15] Z. Yin, S. Li, and F. Tian, "Exact reconstruction method for on-machine measurement of profile," *Precis. Eng.*, vol. 38, no. 4, pp. 969–978, Oct. 2014.
[16] C. Elster, I. Weingärtner, and M. Schulz, "Coupled distance sensor systems for high-accuracy topography measurement: Accounting for scanning stage and systematic sensor errors," *Precis. Eng.*, vol. 30, no. 1, pp. 32–38, Jan. 2006.
[17] M. Schulz, J. Gerhardt, R. D. Geckeler, and C. Elster, "Traceable multiple sensor system for absolute form measurement," *Proc. SPIE*, vol. 5878, Aug. 2005, Art. no. 58780A.
[18] J. Hwang, C.-H. Park, W. Gao, and S.-W. Kim, "A three-probe system for measuring the parallelism and straightness of a pair of rails for ultra-precision guideways," *Int. J. Mach. Tools Manuf.*, vol. 47, nos. 7–8, pp. 1053–1058, Jun. 2007.
[19] W. Gao, J. Yokoyama, H. Kojima, and S. Kiyono, "Precision measurement of cylinder straightness using a scanning multi-probe system," *Precis. Eng.*, vol. 26, no. 3, pp. 279–288, Jul. 2002.
[20] J. J. Yang, X. Chen, G. Q. Ding, L. H. Lei, and Y. Li, "A six-probe scanning method for guide rail straightness measurement," *Appl. Mech. Mater.*, vols. 217–219, pp. 2669–2673, Nov. 2012.
[21] X. Chen, C. Sun, L. Fu, and C. Liu, "A novel reconstruction method for on-machine measurement of parallel profiles with a four-probe scanning system," *Precis. Eng.*, vol. 59, pp. 224–233, Sep. 2019.

XI CHEN received the B.S. degree from the School of Precision Instruments and Optoelectronics Engineering, Tianjin University, in 2015, where she is currently pursuing the Ph.D. degree with the State Key Laboratory of Precision Measuring Technology and Instruments. Her current research interests include geometric measurement, optical measurement technology, and industrial on-line measurement.

CHANGKU SUN received the M.S. degree from the Harbin Institute of Technology, in 1990, and the Ph.D. degree from the Saint Petersburg Precision Mechanics and Optics Institute, Russia, in 1994. He is currently a Professor with the Department of State Key Laboratory of Precision Measuring Technology and Instruments, Tianjin University, and a Visiting Researcher with the Science and Technology on Electro-Optic Control Laboratory, Luoyang Institute of Electro-Optic Equipment. His research interests include machine vision, optical measurement technology, inertial measurement technology, and visual and inertial fusion pose measurement.

LUHUA FU received the M.S. and Ph.D. degrees in power machinery and engineering from Tianjin University, in 1999 and 2004, respectively. She is currently an Associate Professor with the State Key Laboratory of Precision Measuring Technology and Instruments, Tianjin University. Her research interests include geometric measurement, optical measurement technology, and industrial on-line measurement.

CHANGJIE LIU received the M.S. and Ph.D. degrees in precision instrument science and technology from Tianjin University, in 1999 and 2002, respectively. He is currently an Associate Professor with the State Key Laboratory of Precision Measuring Technology and Instruments, Tianjin University. He is also supported by the Program for New Century Excellent Talents in University. His current research interests include visual measurement and guidance, photoelectric detection, and geometric measurement.